Transcriptional regulation of EMT by nuclear MMP28

Nadège Gouignard[1,2], Anne Bibonne[1], Jean-Pierre Saint-Jeannet[2] and Eric Theveneau[1]*

1, Centre de Biologie du Développement (CBD), Centre de Biologie Intégrative (CBI), Université de Toulouse, CNRS, UPS, 118 route de Narbonne 31062, Toulouse Cedex 09, France.

2, New York University, College of Dentistry, Department of Molecular Pathobiology, 345E 24th street, New York NY 10010, USA.

*Corresponding author: eric.theveneau@univ-tlse3.fr

Abstract

Epithelial-Mesenchymal Transition (EMT) is an early event in cell dissemination from epithelial tissues. EMT endows cells with migratory, and sometimes invasive, capabilities and is thus a key process in embryo morphogenesis and cancer progression. So far, Matrix Metalloproteinases (MMPs) have not been considered as key players in EMT but rather studied for their role in matrix remodelling in later events such as cell migration *per se*. Here we used *Xenopus* neural crest cells to assess the role of MMP28 in EMT and migration *in vivo*. We provide strong evidence indicating that MMP28 produced by neighbouring placode cells is imported in the nucleus of neural crest cells for EMT and migration to occur.

Introduction

EMT is a complex process controlled by an array of transcription factors such as members of the *snai*, *twist*, *zeb* and *soxE* families[1,2]. During EMT, cells remodel their adhesion with other cells and the surrounding matrix and display increased cytoskeleton dynamics. These changes drive a change from an apicobasal polarity associated to epithelial stability to a front-rear polarity required for cell migration. EMT is essential for morphogenetic events such as ingression of mesodermal cells during gastrulation or neural crest cells emigration from the neural tube but is also taking place in several diseases such as fibrosis and cancer[1-4]. EMT is an extremely complex and reversible process that is made of a series of non-obligatory steps. Therefore, despite conservation of the core changes taking place at the single cell level, a wealth of regulatory mechanisms has been identified at the molecular level. The way cells undertake EMT appears to be highly context-dependent and renders the task of agreeing on a common definition across fields all the more challenging but common lines are starting to emerge[5].

MMPs are secreted enzymes initially discovered for their ability to remodel the extracellular matrix[6] and early evidence showed that MMPs could influence EMT via their role on the extracellular space[7-9]. Somehow the link between EMT and MMPs was never fully explored. This leads to the current situation where MMPs are not considered as relevant markers or regulators of EMT[5]. However, we now know that MMPs are pleiotropic players in health and diseases that can influence growth, survival and migration[10]. MMPs have numerous non-canonical subcellular localizations (e.g mitochondria, nucleus, cytoplasm) and several unexpected substrates have been described (e.g. cell adhesion molecules, growth factors, guidance cues)[6,11]. These observations suggest numerous putative functions that are not related to the regulation of the extracellular matrix but the functional and physiological relevance of these potential non-canonical functions still awaits demonstration. In particular, it is interesting to note that most MMPs have been detected in the nucleus[12] of at least one cell type and that some have been shown to exhibit transcriptional roles and DNA binding abilities[13,14]. Given the frequent expression of MMPs by cells undergoing EMT, this calls for a re-assessment of their involvement in EMT independently of their effects on extracellular matrix.

Here we used *Xenopus* neural crest cells to assess the putative role of MMP28 in EMT. MMP28 is the latest member of the MMP family. It has a typical MMP structure with a secretion

signal, a pro-domain that needs to be removed for complete enzymatic activity, and a hemopexin-like domain involved in cofactors binding and substrates recognition[15]. Roles and functions of MMP28 are poorly described. It has been shown to be involved in wound healing and nerve repair[15]. It is expressed in pulmonary fibrosis[16] and several human cancers including gastric cancer where it correlates with poor prognosis[17].

Neural crest cells are multipotent stem cells that form at the interface between the neural and non-neural ectoderm[18]. They perform EMT to initiate cell migration and go on to colonize most tissues and organs of the developing embryo[19]. Neural crest EMT relies on oncogenes such as *snai2* and *twist*[20]. The neural crest EMT program is often hijacked by invasive cells during carcinoma progression[21,22] making these cells an extremely relevant *in vivo* model to study EMT. Our data show that, during *Xenopus* development, MMP28 expressed in cranial placodes[23] is required for EMT of neural crest cells. MMP28 is secreted by placode cells, imported into the nucleus of adjacent neural crest cells where its catalytic activity is required for proper implementation of EMT via the maintenance of *twist* expression.

Overall, our results demonstrate a paracrine role for MMP28 in the EMT program of NC cells *in vivo* suggesting that such paracrine role might take place between other cells expressing MMPs such as fibroblasts and cancer cells.

Results

MMP28 is required for the expression of multiple neural crest genes

We found that MMP28, a secreted metalloproteinase, is expressed in cranial placodes adjacent to the cephalic neural crest[23] and given the known importance of neural crest interaction with placodes for normal neural crest migration[24], we decided to assess the putative relevance of MMP28 for neural crest development. MMP28 expression starts before the onset of neural crest migration (Fig. 1a-b) and comparison with markers for neural crest (*sox8* and *snail2*), neural plate (*sox2*) and placodes (*six1*) (Fig. 1b-c) confirms that MMP28 expression is restricted to the posterior part of the pan-placodal domain. MMP28 expression is maintained in placodes at neural crest migration stages (Fig. 1d-e). To assess its functional relevance, we performed loss-of-function experiments using a splice blocking Morpholino directed against MMP28 (MMP28-

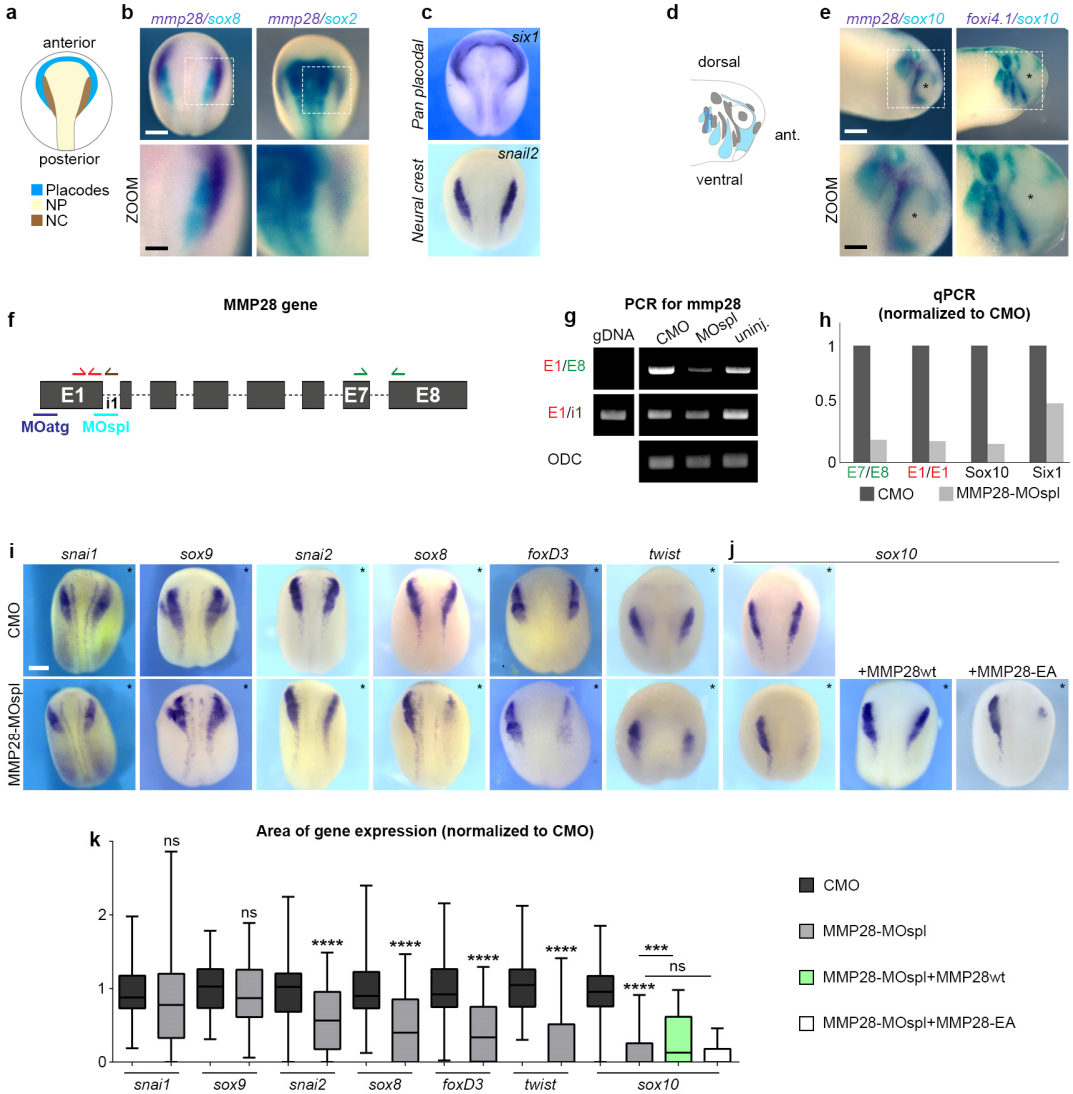

Figure 1. MMP28 expressed in placodes is required for normal expression of neural crest genes
a, Diagram depicting the distribution of placodes, neural crest (NC) and neural plate (NP) at stage 16. **b-c**, *In situ* hybridization for *mmp28*, *sox2, sox8, six1 and snai2,* as indicated. **d**, Diagram depicting the distribution of placodes and neural crest at stage 25. **e**, *In situ* hybridization for *mmp28*, *sox10, and foxi4.1,* as indicated. **f**, diagram of mmp28 gene organization and the relative positions of MMP28 splicing (MOspl) and atg Morpholinos (MOatg) used in this study as well as the position of primers for PCR used to assess MOspl efficiency. **g**, result of PCR with the various combination of primers shown in **f**. **h**, result of qPCR with the various combination of primers shown in **f**, normalized to control MO (CMO). **i-j**, Phenotype of embryos (stage 16) injected with control (CMO) or MMP28 Morpholino (MMP28-MOspl) alone or in combination with wild type (wt) or catalytically dead mutant (EA) MMP28 mRNA and analysed by *in situ* hybridization for *twist* or *sox10* expression (as indicated). **k**, Area of expression of neural crest genes normalized to the non-injected side and CMO condition analysed from six independent experiments. Number of embryos per condition, from left to right: 47, 72; 48, 36; 63, 62; 90, 53; 43, 65, 25, 64; 100, 165, 52, 75). Unpaired t-test with Welch's correction (CMO vs MMP28-MO) for all genes except *sox10.* For *sox10,* ANOVA followed by multiple comparisons, ns $p > 0.1550$, *(MMP28-MO vs MMP28-MO+wt) $p= 0.0292$, ****(CMO vs MMP28-MO) $p < 0.0001$. Scale bar, panels b, c, e and i, 250 µm; zooms, 100 µm.

MOspl) whose efficiency was assessed by RT-PCR and qPCR and translation blocking Morpholino (MMP28-MOatg) (Fig. 1f-h). Knocking down MMP28 led to a severe down

regulation of multiple neural crest genes including *twist*, *sox10*, *snai2*, *sox8* and *foxd3* whereas other genes such as *snai1* and *sox9* were not affected (Fig. 1i-k). Importantly, MMP28 knockdown had no effect on the non-neural ectoderm, the neural plate or the neural plate border gene expression and only marginal effects on placodes themselves with a slight reduction of *six1* expression but no effects on *eya1* or *foxi4.1* (Supplementary Fig. 1). This indicates that, while MMP28 is required for normal expression of multiple neural crest genes, the neural crest territory is still induced and properly positioned in absence of MMP28. *Sox10* being the most affected neural crest gene, we attempted to rescue its expression by co-injecting MMP28-MOspl together with wild-type MMP28 (MMP28wt) or a previously described[15] inactive point mutant version in which the catalytic activity is abolished (MMP28-EA). MMP28wt was sufficient to rescue *sox10* expression in morphant embryos (Fig. 1j and 1k, green bar) whereas MMP28-EA was not (Fig. 1j and 1k, white bar). These data indicate that the catalytic activity of MMP28 secreted by placodes is specifically required for the normal expression of multiple neural crest genes prior to neural crest migration.

MMP28 is required for neural crest EMT and migration

Since inhibition of MMP28 led to a reduction of important EMT regulators such as *twist* and *snai2*, we wanted to assess whether this translated into actual EMT and migration defects. First, we assessed the dorsoventral extension of neural crest streams after MMP28 knockdown and found a severe reduction of the net distance migrated (Fig. 2a-b). Second, we performed *ex vivo* neural crest culture[25] followed by time-lapse imaging to monitor cell dispersion (Fig. 2c-d, Supplementary Movie 1). Neural crest cells taken from embryos injected with a control Morpholino (CMO) extensively moved away from their initial position (Fig. 2c, top panels and 2d), whereas cells coming from embryos in which MMP28 was knocked down failed to disperse (Fig. 2c, bottom panels and 2d, Supplementary Movie 1). Third, we monitored the relative expression of cell adhesion molecules. To initiate migration, *Xenopus* neural crest cells downregulate the expression of E-cadherin and upregulate that of N-cadherin and cadherin-11 to perform contact-inhibition of locomotion[26-28], and rely on α5β1 integrins and cadherin-11 to bind to Fibronectin[28,29]. Therefore, we assessed the expression of these genes in neural crest by qPCR after MMP28 knockdown, using the expression of *mmp28*, *sox10* and *twist* as internal controls

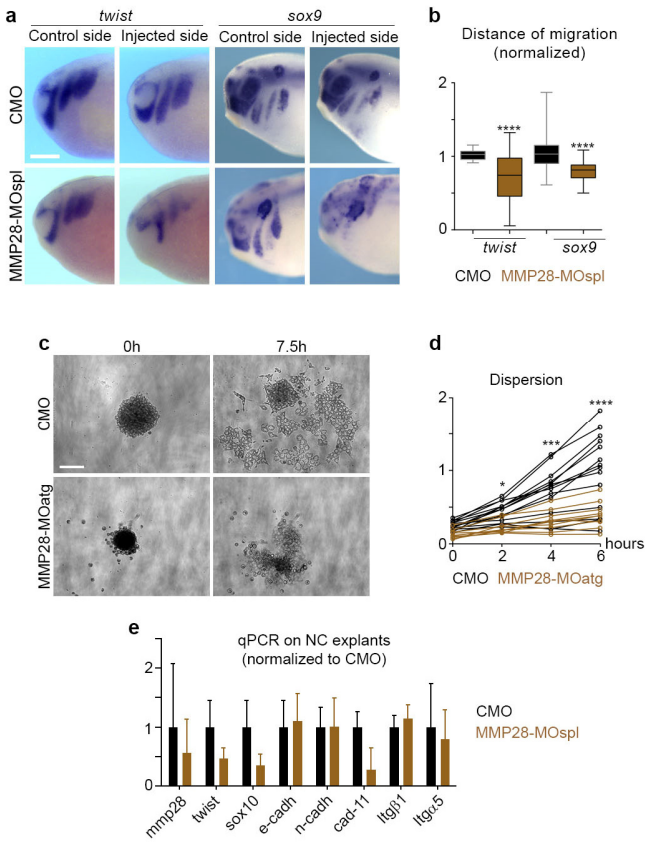

Figure 2. MMP28 is required for normal EMT and cell migration

a, Phenotype of CMO and MMP28-MOspl injected embryos (stage 25) analysed for *twist* and *sox9* expressions, scale bar 250 µm. **b**, Graph plotting the distance migrated by NC cells in CMO and MMP28-MO embryos. t*wist*: nCMO = 22, nMMP28-MO = 46; *sox9*: nCMO = 54, nMMP28-MO = 44. Unpaired t-test, **** $p < 0.0001$. **c**, Representative examples of explants at t0 (one hour after plating on fibronectin) and +7.5h, scale bar 100 µm. **d**, Distribution of explant areas per hour for CMO (n=14) and MMP28-MOatg (n=10). Analysed by two-way ANOVA per time point, CMO vs MMP28MO at t0, ns p=0.26; at t2h, * p=0.433; at t4h, *** p=0.004; at t6h, **** p<0.0001. **e**, Quantitative PCR for expression of *mmp28*, *sox10*, *twist*, *cadherins E*, *N* and *11*, *integrins α5* and *β1* subunits, after injection of MMP28-MOspl or CMO. The values are normalized to *EeF1A1* and to the levels of expression in CMO. From three independent mRNA extractions.

for the MMP28-MO efficiency (Fig. 2e). Injection of the MMP28-MO reduced expression of *mmp28*, *twist* and *sox10* by half. MMP28 knockdown had only mild effects on E and N-cadherins or the α5 and β1 integrin subunits while it severely reduced the expression of cadherin-11 indicating that MMP28-MO neural crest cells initiate EMT but fail to complete it (Fig. 2e). Altogether, these three independent analyses show that the inhibition of EMT transcription factors under MMP28 knockdown conditions translates into EMT and migration defects at tissue (Fig. 2a-b), cellular (Fig. 2c-d) and molecular (Fig. 2e) levels.

Twist expression is sufficient to rescue MMP28 knockdown

Given that the expressions of Twist, an upstream regulator of EMT, and cadherin-11, a downstream effector of the EMT cascade, are severely affected by MMP28 knockdown we wondered whether forcing expression of either these genes might be sufficient to rescue MMP28 knockdown phenotype. For that, we co-injected MMP28-MOspl with the mRNA for *twist* or

cadherin-11 (Fig. 3a-c). Embryos injected with the control MO displayed normal neural crest migration on both the uninjected and the injected side while embryos injected with MMP28-MOspl had impaired neural crest migration on the injected side. Interestingly, co-injection with *twist* mRNA was sufficient to partially restore dorso-ventral neural crest migration while co-injection of *cadherin-11* mRNA was not (Fig. 3b-c).

To better understand how these treatments affected neural crest cells we plated the various conditions onto Fibronectin. First, we let explants migrate for 3 hours and fixed them for nuclear and actin staining with DAPI and Phalloidin (Fig. 3d-f). We then counted the number of explants that were still attached after fixation, washes and the staining procedure. Fig. 3e shows a low magnification of each well with adhering explants outlined in purple and detached explants outlined in yellow. In control MO conditions and MMP28-MO+Twist mRNA, all explants remained attached whereas after MMP28 knockdown only 5 out of 12 explants had a significant amount of cells left attached to the dish. Interestingly, in the MMP28-MO+Cadherin-11 mRNA, 8 out of 10 explants remained attached to the substrate (Fig 3e-f). We next looked at cell morphology. Cells injected with control MO or MMP28-MO together with Twist or Cadherin-11 were able to flatten on the substrate and to form protrusions while MMP28-MO cells were mostly round and poorly protrusive (Fig. 3g). We measured the area of protrusions either directed toward a free space (Fig. 3h, outward protrusions) or in between cells (Fig. 3h, cryptic protrusions). Twist and Cadherin-11 mRNA were each sufficient to rescue protrusive activity in MMP28-MO cells (Fig. 3h).

Next, we assessed cells dynamics by time-lapse imaging (Fig. 3d, 1i-k, Supplementary Movie 2). Cells injected with control MO dispersed normally (Fig. 3i-k, black graphs and curves) while MMP28-MO cells were round and failed to significantly disperse (Fig. 3i-k, brown graphs and curves). Interestingly, Twist expression was able to restore normal dispersion of MMP28-MO injected neural crest cells (Fig. 3i-k, blue graphs and curves) but not that of Cadherin-11 (Fig. 3i-k, pink graphs and curves). Altogether, these data indicate that Twist and Cadherin-11 are essential players downstream of MMP28. Cadherin-11 is sufficient to restore cell-matrix adhesion but this rescue of adhesion does not translate into an efficient rescue of cell motility *in* or *ex vivo*. By contrast, Twist expression fully restores adhesion and dispersion *ex vivo* and significantly restores neural crest migration *in vivo*.

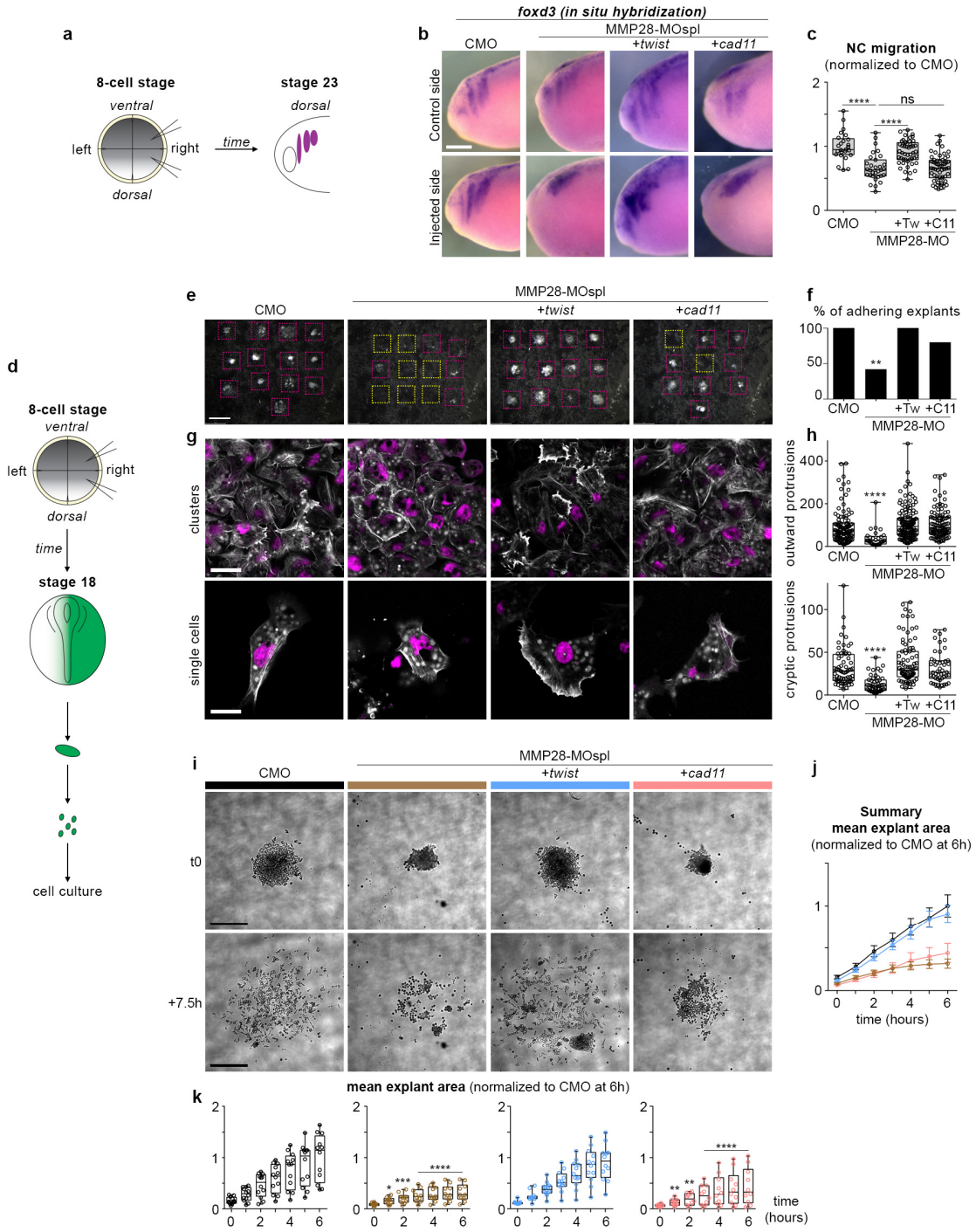

Figure 3. Twist expression is sufficient to rescue adhesion and migration of neural crest cells

a, diagram depicting the experimental set-up with injection of MO and mRNA in two blastomeres on one side of 8-cell stage embryos left to develop until neural crest migration stage. **b**, *in situ* hybridization against foxd3 following injection with CMO, MMP28-MOspl or the co-injection of MMP28-MOspl with *twist* and *cadherin-11* mRNA. **c**, Graph plotting the distance migrated by neural crest cells in the experimental conditions shown in **b**, nCMO = 25, nMMP28-MOspl = 31 nMMP28-MOspl+*twist* = 57, nMMP28-MOspl+*cad11* = 47 from two independent experiments. ANOVA followed by uncorrected Fisher's LSD; ****, p <

0.0001, ns, p = 0.8829. **d**, diagram depicting the experimental procedure for neural crest culture on Fibronectin. **e**, low magnification images of explants in all experimental conditions after fixation, washes and the staining procedure. Adhering explants are outlined in purple, detached explants are outlined in yellow; scale bar, 500 µm. **f**, quantification of adhering explants, CMO = 13/13; MMP28-MOspl = 5/13; MMP28-MOspl+*twist* = 12/12; MO28-MOspl+*cad11* = 8/10. Contingency tables for the comparison of proportion; CMO vs MMP28-MOspl, T=10.53, alpha 0.01 (**), MMP28-MOspl vs MMP28-MOspl+*twist*, T=9.88, alpha 0.01 (**), MMP28-MOspl vs MMP28-MOspl+*cad11*, T=3.31 (ns), CMO vs MMP28-MOspl+*cad11*, T=2.85, (ns). **g**, DAPI (magenta) and Phalloidin (white) staining; scale bars, 40µm for clusters, 20µm for single cells. **h**, protrusion area in µm², outward protrusions nCMO = 64, nMMP28-MOspl = 49, nMOspl+*twist* = 47, nMOspl+*cad11* = 87; cryptic protrusions nCMO = 103, nMMP28-MOspl = 29, nMOspl+*twist* = 140, nMOspl+Cad11 = 100; ANOVA, Kruskal-Wallis test; ****, p < 0.0001. **i**, time-lapse imaging of neural crest explants, scale bar, 250µm. **j**, summary graph with curves showing the mean area and standard deviation per experimental condition shown in **i** per time point. **k**, mean explant area + s.d. per explant per conditions shown in **i** per time point, nCMO = 12, nMMP28-MOspl = 10, nMOspl+*twist* = 12, nMOspl+*cad11* = 10.

MMP28 can traffic to the nucleus of neural crest cells

Newt, we wondered how MMP28 might affect the expression of neural crest genes while being produced by adjacent placodes. Despite being secreted several MMPs, including MMP28[16], have been detected in the nucleus of various cell types[12,16]. Thus, we analysed the amino acid sequence of *Xenopus* MMP28 for putative nuclear export and nuclear localization signals (NES/NLS). We found 2 putative NES and 2 putative NLS sites in MMP28 (Fig. 4a). To test whether MMP28 is able to traffic to the nucleus, we expressed a GFP-tagged version of MMP28 in *Xenopus* embryos, harvested embryos and performed cell fractionation followed by western blot (Fig. 4b). We found MMP28 in the membrane (Mem), the soluble cytosol (Cy) and the cytoskeleton-associated (CytoSK) fractions as well as the soluble (Sol) and chromatin-associated (Chr) nuclear fractions (Fig. 4b). To substantiate these data, we expressed MMP28-GFP in neural crest cells and performed 3D confocal imaging (Fig. 4c, Supplementary Movie 3). Nuclei were counterstained with DAPI and the DAPI signal used as a mask to probe the amount of GFP signal embedded within it. Multiple GFP spots were detected in the nuclei of neural crest cells (Fig. 4c, zooms). To assess whether the addition of the GFP-tag might be responsible for a non-specific nuclear accumulation of MMP28, we performed the same experiment with a flag-tagged version of MMP28. MMP28-flag was also detected in the neural crest nuclei excluding the possibility that the GFP tag non-specifically drives MMP28 nuclear accumulation (Supplementary Movie 4).

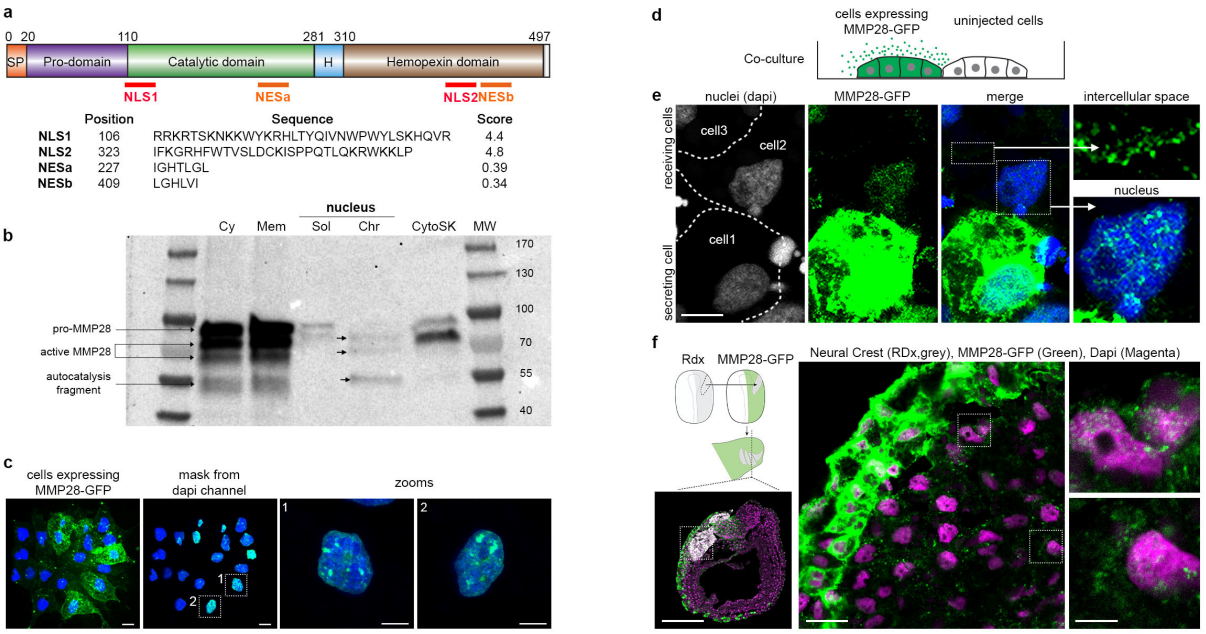

Figure 4. MMP28 can travel from the ectoderm to the nucleus of neural crest cells in vivo

a, diagram of MMP28 protein structure and relative position, sequence and score of the putative NLS and NES signals identified by bioinformatics (see methods). **b,** western blot against GFP after cell fractionation from embryos expressing MMP28-GFP; Cy, cytosol; Mem, membrane; Sol, soluble nuclear fraction; Chr, chromatin-bound nuclear fraction; CytoSK, cytoskeleton fraction; MW, molecular weight. **c**, neural crest explant expressing MMP28-GFP observed by 3D confocal imaging, scales bars 10 µm. **d,** diagram depicting the co-culture assay. **e**, Control *Xenopus* neural crest cells and neural crest cells expressing MMP28-GFP co-cultured on Fibronectin, immunostained with anti-GFP antibody (green) and counterstained by DAPI (blue), representative images from two independent experiments with 6 explants, scale bar 10 µm. **f**, Upper left panel, diagram depicting the grafting procedure. Neural crest from a donor embryo labelled with rhodamine dextran (grey) were grafted into a host embryo expressing MMP28-GFP in the ectoderm. Section of grafted embryo immunostained with anti-GFP antibody (green) and counterstained with DAPI (magenta), scale bar 250 µm. Dash line squares indicate zoomed areas, scale bar left panel 500 µm, middle panel 50 µm, right panel 5 µm.

MMP28 produced by placodes can be imported into neural crest cells' nuclei

In vivo, MMP28 is not expressed by neural crest cells but by nearby placodes. Therefore, to test whether MMP28 can traffic to neighbouring cells in a paracrine manner, we co-cultured control neural crest cells and neural crest cells expressing MMP28-GFP. We detected MMP28-GFP in the intercellular space between expressing and non-expressing cells as well as in the nucleus of non-expressing cells (Fig. 4d-e). We next tested whether MMP28 could travel from placodes to neural crest cells *in vivo* within a time window compatible with normal neural crest-

placodes interactions. To do so, we expressed MMP28-GFP in the ectoderm of *Xenopus* embryos and grafted neural crest explants labelled with rhodamine-dextran as a tracer (Fig. 4f). Embryos were fixed 4 hours after the graft and processed for histology and confocal imaging. MMP28-GFP was detected in the cytoplasm and the nucleus of multiple neural crest cells located underneath the MMP28-positive ectoderm, including nuclei that were several cell diameters away from the ectoderm. These data show that MMP28 can traffic to travel from the ectoderm, where placodes are located, to the nuclei of neural crest cells within a few hours *in vivo*.

Active MMP28 is required within the nuclei of neural crest cells for normal *twist* expression

To determine whether the nuclear localization was required for MMP28 function, we designed versions of MMP28 that would be either prevented from accumulating in the nucleus, by adding a strong NES signal or sequestered in the nucleus. For the later, we removed the secretion peptide (ΔSP) and added a strong NLS. We confirmed that the $MMP28^{NES}$ and $MMP28^{\Delta SPNLS}$ localized to the expected cellular compartments (Fig. 5a-b). Since MMPs are usually activated by removal of their pro-domain while passing through the Golgi[30], we assessed whether deletion of the secretion peptide might affect removal of the pro-domain. We compared the profiles of MMP28wt, $MMP28^{\Delta SP}$ and $MMP28^{\Delta SP/NLS}$ in the soluble and chromatin-associated nuclear fractions by western blot. Indeed, preventing entry into the secretion pathway inhibited removal of the pro-domain (Supplementary Fig. 2). We then used the NES and ΔSPNLS versions of MMP28 to attempt to rescue MMP28 knockdown *in vivo*. $MMP28^{NES}$ was not able to rescue *sox10* or *twist* expression in contrast to the nuclear version of MMP28 (fig. 5c-d). Given that the ΔSPNLS form still has its pro-domain, this result would suggest that the catalytic activity may not be required for MMP28 function in the nucleus. However, pro-MMPs have basal catalytic activity and can be further activated by a change of conformation known as an allosteric activation[30,31]. Therefore, the rescue obtained with the ΔSPNLS form is not a definitive proof that catalytic activity is dispensable in the nucleus. To address this point, we generated a catalytically inactive version of the ΔSPNLS ($MMP28^{EA/\Delta SPNLS}$). Importantly, this catalytically inactive form of MMP28 was not able to rescue MMP28 knockdown (Fig. 5c-d) indicating that the catalytic activity of MMP28 is indeed required within the nucleus.

Altogether, our data indicate that active MMP28 produced by the placode cells needs to be imported into the nucleus of neural crest cells for normal Twist-dependent EMT and migration to occur (Fig. 5e).

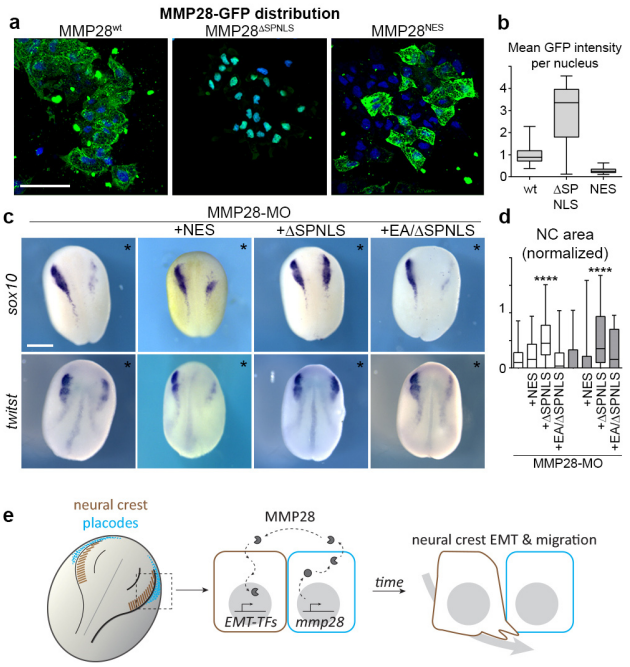

Figure 5. Active nuclear MMP28 is required for the expression of *twist*

a, neural crest expressing GFP-tagged versions of MMP28wt, MMP28$^{\Delta SPNLS}$ and MMP28^{NES} cultured on fibronectin, scale bar 100 µm. **b**, Mean intensity of the GFP signal per nucleus from 3D confocal stacks normalized to mean intensity of MMP28-GFPwt, nWT = 85 from three explants, nΔSPNLS = 39 from two explants, nNES = 206 from two explants. **c**, Phenotype of MMP28-MO injected embryos co-injected with MMP28^{NES}-GFP, MMP28$^{\Delta SPNLS}$-GFP or MMP28$^{EA/SPNLS}$-GFP and analysed for *twist* and *sox10* expression, scale bar 250 µm. Asterisks mark injected side. **d**, Area of NC gene expression normalized to non-injected side from 7 independent experiments. Number of embryos per condition, from left to right: 137, 47, 94, 28, 60, 49, 70, 18. ANOVA followed by multiple comparisons, **** $p < 0.0001$. **e**, Diagram of a dorsal view of a *Xenopus* embryo with neural crest in brown and placodes in cyan. MMP28 from placodes is imported into neural crest's nuclei to promote EMT.

Discussion

We found that MMP28 is produced by cranial placodes but acts on neural crest cells. Interestingly, these two cell populations jointly form the cranial peripheral nervous system[32] and are already known to depend on one another for their normal development. Normal neural crest migration along the dorsoventral axis and patterning in discrete streams requires interactions with placodes on multiple levels. Placodes are the source of positive and negative regulators of neural crest migration such as Sdf1/CXCL12 and class3-semaphorins[33-35]. Direct physical interaction between neural crest and placodes via N-cadherin-dependent heterotypical contact-inhibition of locomotion drives the redistribution of placodal cells throughout the head which in turn helps splitting the neural crest population in streams[24,36]. These neural crest-placodes interactions are not specific to *Xenopus* development and are found in other vertebrates with some degree of conservation in terms of molecular and cellular mechanisms[37-40]. MMP28 acts earlier than the

previously identified mechanisms linking neural crest and placodes development. While physical interactions and secreted guidance cues directly influence cell motility and adhesion during migration, MMP28 expression in placodes starts at around stage 14 which is after the expression of *snai2*, *sox8*, *foxd3* and *twist* and concomitant with that of *Sox10*. All of which are decreased in absence of MMP28. These data indicate a new level of control between these two cell populations such that the neural crest EMT program is maintained only if MMP28 is secreted from the placodes. This also raises the possibility that while MMP28 is expressed from very early stages of *Xenopus* development[23], its increased expression in the neural crest domain prior to EMT might be promoted by neural crest EMT-TFs themselves, adding yet another feedback loop in the neural crest gene regulatory network.

We found that MMP28 is imported as an active enzyme in the nuclei of neural crest cells. How is this possible? First of all, more than half of all MMPs have been detected in the nucleus of at least one cell type[12], including MMP28[16], indicating that the ability to traffic to the nucleus is a conserved property of MMPs. Putative nuclear localization signals have been found in MMP3 and its ability to go from extracellular space to the nucleus to participate to transcription has been shown in cell culture[14]. MMP14 (a.k.a MT1-MMP) can go to the nucleus and contributes to the transcriptional activation of PI3K in cultured mouse primary macrophages[13]. In this study, the authors showed that the transmembrane domain of MMP14 is needed for nuclear import to occur. However, a deletion construct lacking both the secretion signal and the transmembrane domain produced directly in the cytoplasm can be imported into the nucleus. Further, direct DNA binding to the promoter of PI3K was demonstrated as well as the ability of MMP14 to activate a minimal promoter sequence. Unfortunately, the mechanisms and cofactors involved in controlling entry of MMPs into the cell and their subsequent nuclear import are still unknown and will required extensive work to be elucidated.

MMP28 expression has been described during wound healing[41]. Interestingly, its expression is not found in front cells located near the wound but in proliferative cells located several rows behind the gap that needs to be filled and does not overlap with other proteases[42]. It would be interesting to assess whether MMP28 acts in paracrine manner similar to what we found in neural crest. In cancer, MMP28 is detected in numerous tumour types. MMP28 promotes cell proliferation in oral squamous cell carcinoma[43] while in gastric cancer[17] and

hepatocellular carcinoma[44] (HCC) there is a clear association with poor prognosis. In HCC cell lines, MMP28 overexpression promotes EMT via activation of *zeb1* and *zeb2* downstream of the Notch pathway[44]. Given that MMP28 was previously shown to favour EMT via an extracellular effect on the TGFβ pathway in lung carcinoma cell lines[9], the authors of the HCC study did not investigate whether MMP28 could act directly from within the cells.

In conclusion, given i) the conserved ability of MMPs to traffic to the nucleus, ii) the few examples of DNA binding and transcriptional activities previously described, and iii) the frequent expression of MMPs in cells undergoing EMT, we propose that the role of MMPs in the transcriptional regulation of EMT might be a conserved feature and would need to be systematically assessed.

References

1 Brabletz, T., Kalluri, R., Nieto, M. A. & Weinberg, R. A. EMT in cancer. *Nature reviews. Cancer* **18**, 128-134, doi:10.1038/nrc.2017.118 (2018).

2 Nieto, M. A., Huang, R. Y., Jackson, R. A. & Thiery, J. P. Emt: 2016. *Cell* **166**, 21-45, doi:10.1016/j.cell.2016.06.028 (2016).

3 Thiery, J. P. & Lim, C. T. Tumor dissemination: an EMT affair. *Cancer cell* **23**, 272-273, doi:10.1016/j.ccr.2013.03.004 (2013).

4 Lim, J. & Thiery, J. P. Epithelial-mesenchymal transitions: insights from development. *Development* **139**, 3471-3486, doi:10.1242/dev.071209 (2012).

5 Yang, J. *et al.* Guidelines and definitions for research on epithelial-mesenchymal transition. *Nature reviews. Molecular cell biology* **21**, 341-352, doi:10.1038/s41580-020-0237-9 (2020).

6 Iyer, R. P., Patterson, N. L., Fields, G. B. & Lindsey, M. L. The history of matrix metalloproteinases: milestones, myths, and misperceptions. *American journal of physiology. Heart and circulatory physiology* **303**, H919-930, doi:10.1152/ajpheart.00577.2012 (2012).

7 Sternlicht, M. D. *et al.* The stromal proteinase MMP3/stromelysin-1 promotes mammary carcinogenesis. *Cell* **98**, 137-146 (1999).

8 Radisky, D. C. *et al.* Rac1b and reactive oxygen species mediate MMP-3-induced EMT and genomic instability. *Nature* **436**, 123-127, doi:10.1038/nature03688 (2005).

9 Illman, S. A., Lehti, K., Keski-Oja, J. & Lohi, J. Epilysin (MMP-28) induces TGF-beta mediated epithelial to mesenchymal transition in lung carcinoma cells. *Journal of cell science* **119**, 3856-3865, doi:10.1242/jcs.03157 (2006).

10 Bonnans, C., Chou, J. & Werb, Z. Remodelling the extracellular matrix in development and disease. *Nature reviews. Molecular cell biology* **15**, 786-801, doi:10.1038/nrm3904 (2014).

11 Jobin, P. G., Butler, G. S. & Overall, C. M. New intracellular activities of matrix metalloproteinases shine in the moonlight. *Biochim Biophys Acta Mol Cell Res* **1864**, 2043-2055, doi:10.1016/j.bbamcr.2017.05.013 (2017).

12 Mannello, F. & Medda, V. Nuclear localization of matrix metalloproteinases. *Prog Histochem Cytochem* **47**, 27-58, doi:10.1016/j.proghi.2011.12.002 (2012).

13 Shimizu-Hirota, R. *et al.* MT1-MMP regulates the PI3Kdelta.Mi-2/NuRD-dependent control of macrophage immune function. *Genes & development* **26**, 395-413, doi:10.1101/gad.178749.111 (2012).

14 Eguchi, T. *et al.* Novel transcription-factor-like function of human matrix metalloproteinase 3 regulating the CTGF/CCN2 gene. *Molecular and cellular biology* **28**, 2391-2413, doi:10.1128/MCB.01288-07 (2008).

15 Rodgers, U. R. *et al.* Expression and function of matrix metalloproteinase (MMP)-28. *Matrix biology : journal of the International Society for Matrix Biology* **28**, 263-272, doi:10.1016/j.matbio.2009.04.006 (2009).

16 Maldonado, M. *et al.* Upregulation and Nuclear Location of MMP28 in Alveolar Epithelium of Idiopathic Pulmonary Fibrosis. *American journal of respiratory cell and molecular biology* **59**, 77-86, doi:10.1165/rcmb.2017-0223OC (2018).

17 Zhang, J. *et al.* Overexpression of MMP21 and MMP28 is associated with gastric cancer progression and poor prognosis. *Oncology letters* **15**, 7776-7782, doi:10.3892/ol.2018.8328 (2018).

18 Mayor, R. & Theveneau, E. The neural crest. *Development* **140**, 2247-2251, doi:10.1242/dev.091751 (2013).

19 Le Douarin, N. M. & Dupin, E. The neural crest in vertebrate evolution. *Current opinion in genetics & development* **22**, 381-389, doi:10.1016/j.gde.2012.06.001 (2012).
20 Gouignard, N., Andrieu, C. & Theveneau, E. Neural crest delamination and migration: Looking forward to the next 150 years. *Genesis*, e23107, doi:10.1002/dvg.23107 (2018).
21 Kerosuo, L. & Bronner-Fraser, M. What is bad in cancer is good in the embryo: importance of EMT in neural crest development. *Seminars in cell & developmental biology* **23**, 320-332, doi:10.1016/j.semcdb.2012.03.010 (2012).
22 Theveneau, E. & Mayor, R. Neural crest delamination and migration: from epithelium-to-mesenchyme transition to collective cell migration. *Developmental biology* **366**, 34-54, doi:10.1016/j.ydbio.2011.12.041 (2012).
23 Gouignard, N., Theveneau, E. & Saint-Jeannet, J. P. Dynamic expression of MMP28 during cranial morphogenesis. *Phil Trans R Soc Lond B Biol Sci. (IN PRESS)* **IN PRESS**, doi:https://doi.org/10.1101/850834 (2020).
24 Theveneau, E. *et al.* Chase-and-run between adjacent cell populations promotes directional collective migration. *Nature cell biology* **15**, 763-772, doi:10.1038/ncb2772 (2013).
25 Gouignard, N., Rouviere, C. & Theveneau, E. Using Xenopus Neural Crest Explants to Study Epithelial-Mesenchymal Transition. *Methods in molecular biology* **2179**, 257-274, doi:10.1007/978-1-0716-0779-4_20 (2021).
26 Scarpa, E. *et al.* Cadherin Switch during EMT in Neural Crest Cells Leads to Contact Inhibition of Locomotion via Repolarization of Forces. *Developmental cell* **34**, 421-434, doi:10.1016/j.devcel.2015.06.012 (2015).
27 Becker, S. F., Mayor, R. & Kashef, J. Cadherin-11 mediates contact inhibition of locomotion during Xenopus neural crest cell migration. *PloS one* **8**, e85717, doi:10.1371/journal.pone.0085717 (2013).
28 Langhe, R. P. *et al.* Cadherin-11 localizes to focal adhesions and promotes cell-substrate adhesion. *Nature communications* **7**, 10909, doi:10.1038/ncomms10909 (2016).
29 Alfandari, D., Cousin, H., Gaultier, A., Hoffstrom, B. G. & DeSimone, D. W. Integrin alpha5beta1 supports the migration of Xenopus cranial neural crest on fibronectin. *Developmental biology* **260**, 449-464 (2003).
30 Hadler-Olsen, E., Fadnes, B., Sylte, I., Uhlin-Hansen, L. & Winberg, J. O. Regulation of matrix metalloproteinase activity in health and disease. *The FEBS journal* **278**, 28-45, doi:10.1111/j.1742-4658.2010.07920.x (2011).
31 Ra, H. J. & Parks, W. C. Control of matrix metalloproteinase catalytic activity. *Matrix biology : journal of the International Society for Matrix Biology* **26**, 587-596, doi:10.1016/j.matbio.2007.07.001 (2007).
32 Theveneau, E. & Mayor, R. Collective cell migration of the cephalic neural crest: the art of integrating information. *Genesis* **49**, 164-176, doi:10.1002/dvg.20700 (2011).
33 Bajanca, F. *et al.* In vivo topology converts competition for cell-matrix adhesion into directional migration. *Nature communications* **10**, 1518, doi:10.1038/s41467-019-09548-5 (2019).
34 Theveneau, E. *et al.* Collective chemotaxis requires contact-dependent cell polarity. *Developmental cell* **19**, 39-53, doi:10.1016/j.devcel.2010.06.012 (2010).
35 Yu, H. H. & Moens, C. B. Semaphorin signaling guides cranial neural crest cell migration in zebrafish. *Developmental biology* **280**, 373-385, doi:10.1016/j.ydbio.2005.01.029 (2005).
36 Szabó, A., Theveneau, E., Turan, M. & Mayor, R. Neural crest streaming as an emergent property of tissue interactions during morphogenesis. *PLoS computational biology* **15**, e1007002, doi:10.1371/journal.pcbi.1007002 (2019).

37 Culbertson, M. D., Lewis, Z. R. & Nechiporuk, A. V. Chondrogenic and gliogenic subpopulations of neural crest play distinct roles during the assembly of epibranchial ganglia. *PloS one* **6**, e24443, doi:10.1371/journal.pone.0024443 (2011).
38 Freter, S., Fleenor, S. J., Freter, R., Liu, K. J. & Begbie, J. Cranial neural crest cells form corridors prefiguring sensory neuroblast migration. *Development* **140**, 3595-3600, doi:10.1242/dev.091033 (2013).
39 Golding, J. P., Trainor, P., Krumlauf, R. & Gassmann, M. Defects in pathfinding by cranial neural crest cells in mice lacking the neuregulin receptor ErbB4. *Nature cell biology* **2**, 103-109, doi:10.1038/35000058 (2000).
40 Escot, S., Blavet, C., Hartle, S., Duband, J. L. & Fournier-Thibault, C. Misregulation of SDF1-CXCR4 signaling impairs early cardiac neural crest cell migration leading to conotruncal defects. *Circulation research* **113**, 505-516, doi:10.1161/CIRCRESAHA.113.301333 (2013).
41 Illman, S. A., Lohi, J. & Keski-Oja, J. Epilysin (MMP-28)--structure, expression and potential functions. *Experimental dermatology* **17**, 897-907, doi:10.1111/j.1600-0625.2008.00782.x (2008).
42 Saarialho-Kere, U. *et al.* Epilysin (MMP-28) expression is associated with cell proliferation during epithelial repair. *The Journal of investigative dermatology* **119**, 14-21, doi:10.1046/j.1523-1747.2002.01790.x (2002).
43 Lin, M. H., Liu, S. Y., Su, H. J. & Liu, Y. C. Functional role of matrix metalloproteinase-28 in the oral squamous cell carcinoma. *Oral oncology* **42**, 907-913, doi:10.1016/j.oraloncology.2005.12.012 (2006).
44 Zhou, J. *et al.* Upregulated MMP28 in Hepatocellular Carcinoma Promotes Metastasis via Notch3 Signaling and Predicts Unfavorable Prognosis. *International journal of biological sciences* **15**, 812-825, doi:10.7150/ijbs.31335 (2019).
45 Mayor, R., Morgan, R. & Sargent, M. G. Induction of the prospective neural crest of Xenopus. *Development* **121**, 767-777 (1995).
46 Hopwood, N. D., Pluck, A. & Gurdon, J. B. A Xenopus mRNA related to Drosophila twist is expressed in response to induction in the mesoderm and the neural crest. *Cell* **59**, 893-903 (1989).
47 Monsoro-Burq, A. H., Fletcher, R. B. & Harland, R. M. Neural crest induction by paraxial mesoderm in Xenopus embryos requires FGF signals. *Development* **130**, 3111-3124, doi:10.1242/dev.00531 (2003).
48 Essex, L. J., Mayor, R. & Sargent, M. G. Expression of Xenopus snail in mesoderm and prospective neural fold ectoderm. *Developmental dynamics : an official publication of the American Association of Anatomists* **198**, 108-122, doi:10.1002/aja.1001980205 (1993).
49 O'Donnell, M., Hong, C. S., Huang, X., Delnicki, R. J. & Saint-Jeannet, J. P. Functional analysis of Sox8 during neural crest development in Xenopus. *Development* **133**, 3817-3826, doi:10.1242/dev.02558 (2006).
50 Spokony, R. F., Aoki, Y., Saint-Germain, N., Magner-Fink, E. & Saint-Jeannet, J. P. The transcription factor Sox9 is required for cranial neural crest development in Xenopus. *Development* **129**, 421-432 (2002).
51 Aoki, Y. *et al.* Sox10 regulates the development of neural crest-derived melanocytes in Xenopus. *Developmental biology* **259**, 19-33, doi:10.1016/S0012-1606(03)00161-1 (2003).
52 David, R., Ahrens, K., Wedlich, D. & Schlosser, G. Xenopus Eya1 demarcates all neurogenic placodes as well as migrating hypaxial muscle precursors. *Mechanisms of development* **103**, 189-192, doi:10.1016/s0925-4773(01)00355-0 (2001).

53 Ghanbari, H., Seo, H. C., Fjose, A. & Brandli, A. W. Molecular cloning and embryonic expression of Xenopus Six homeobox genes. *Mechanisms of development* **101**, 271-277, doi:10.1016/s0925-4773(00)00572-4 (2001).
54 Schlosser, G. & Ahrens, K. Molecular anatomy of placode development in Xenopus laevis. *Developmental biology* **271**, 439-466, doi:10.1016/j.ydbio.2004.04.013 (2004).
55 Mizuseki, K., Kishi, M., Matsui, M., Nakanishi, S. & Sasai, Y. Xenopus Zic-related-1 and Sox-2, two factors induced by chordin, have distinct activities in the initiation of neural induction. *Development* **125**, 579-587 (1998).
56 Jonas, E., Sargent, T. D. & Dawid, I. B. Epidermal keratin gene expressed in embryos of Xenopus laevis. *Proceedings of the National Academy of Sciences of the United States of America* **82**, 5413-5417, doi:10.1073/pnas.82.16.5413 (1985).
57 Bang, A. G., Papalopulu, N., Kintner, C. & Goulding, M. D. Expression of Pax-3 is initiated in the early neural plate by posteriorizing signals produced by the organizer and by posterior non-axial mesoderm. *Development* **124**, 2075-2085 (1997).
58 Taillard, E. D., Waelti, P. & Zuber, J. Few statistical tests for proportions comparison. *Eur J Oper Res* **185**, 1336-1350, doi:10.1016/j.ejor.2006.03.070 (2008).
59 Kosugi, S., Hasebe, M., Tomita, M. & Yanagawa, H. Systematic identification of cell cycle-dependent yeast nucleocytoplasmic shuttling proteins by prediction of composite motifs. *Proceedings of the National Academy of Sciences of the United States of America* **106**, 10171-10176, doi:10.1073/pnas.0900604106 (2009).
60 Fu, S. C., Huang, H. C., Horton, P. & Juan, H. F. ValidNESs: a database of validated leucine-rich nuclear export signals. *Nucleic acids research* **41**, D338-343, doi:10.1093/nar/gks936 (2013).

Methods

Xenopus manipulation and in vitro fertilization

All experiments using *Xenopus laevis* were performed in accordance with the guidelines of the Guide for the Care and Use of Laboratory Animals of the National Institutes of Health, and were approved by the Institutional Animal Care and Use Committee of New York University (animal protocol # IA16-00052) or institutional and national guidelines, under the institutional licence number A 31 55501 delivered by the Préfecture de la Haute-Garonne. Female *Xenopus* laevis were injected with 750 to 1000 International Units of Chorionic Gonadotrophin (hCG, Chorulon) and kept overnight at 18°C. Male *Xenopus laevis* were euthanized in 3g/L Tricaine (Millipore Sigma E10521) and the testis immediately collected and kept in L15 medium (Millipore Sigma L5520) at 4ºC. For fertilization, a suspension of minced testis was added to the oocytes collected in petri dish in 0.1X Normal Amphibian Medium (NAM): NaCl (110mM), KCl (2mM), Ca(CO3)2 (1mM), MgSO4 (1mM), EDTA (0.1mM), NaHCO3 (1mM), Sodium Phosphate (2mM).

Expression vectors and Morpholinos for MMP28

MMP28pCMV-SPORT6 clone was purchased from OpenBiosystems (Horizon Discovery/Dharmacon, #MXL1736-92024189). MMP28 open reading frame was amplified by PCR using the following primers, MMP28_pCS2_fdw: ATCGATATGGAAGCTGATATTCCATC MMP28_pCS2+_rev: CTCGAGTCAAGTCACATCATTTTTACA, and cloned into a pCS2+ backbone. MMP28^{wt}-GFP was produced from MMP28^{wt}-pCS2 by adding a GFP sequence using a PCR strategy with primers eGFP_pCS2_fdw: 5'-AAGGATGCAACTAGGATCCGCTCGATGAGCAAGGGCG-'3, eGFP_pCS2_rev: 5'-CGACTCACTATAGTTCTAGACTTACTTGTA-3' and BamHI/XbaI cloning. MMP28$^{\Delta SP/NLS}$-GFP-pCS2 was synthetized by Genescript®. MMP28$^{\Delta SP/wt}$-GFP-pCS2 was produced from MMP28$^{\Delta SP/NLS}$-GFP-pCS2 by excision of the NLS sequence (BamHI/XhoI). MMP28^{NES2}-GFP was derived from MMP28^{wt}-GFP by insertion in SpeI site of the sequence 5'-CTGGCCCTGAAGCTGGCCGGCCTGGACATCGGCAGC-3' using oligo annealing procedure. The catalytically dead mutants MMP28^{EA}-pCS2 and MMP28$^{EA\text{-}\Delta SP/NLS}$-GFP-pCS2 were produced by point mutation of Glutamic acid^{226} to Alanine from MMP28^{wt}pCS2 and Glutamic acid^{209} to Alanine from MMP28$^{\Delta SP/NLS}$-GFP-pCS2 using QuikChange II site-Directed Mutagenesis Kit (Agilent #200523) with the primers MMP28_E-A_fdw: 5'-ACTGGCACATGCGATTGGACAT-3' and MMP28_E-A_rev: 5'-ATGTCCAATCGCATGTGCCAGT-3'. Morpholino antisense oligonucleotides were purchased from Gene-Tools (Pilomath, OR): MMP28-MOspl: 5'-GTATGCCTCTGATATTTACCTGTGC-3', MMP28-MOatg: 5'-TGTTTAATGGATGAGTAACTTATCT -3' and Control MO (CMO): 5'-CCTCTTACCTCAGTTACAATTTATA-3'.

Microinjections

mRNAs were synthesized *in vitro* from the various pCS2 constructs using the Ambion Message Machine kit (Austin, TX). MMP28^{wt} and MMP28^{EA} mRNAs were injected at 8-cell stage in two animal blastomeres at 600 pg/bl, while all MMP28-GFP mRNAs were injected at 900 pg/bl to respect equimolarity. CMO and MMP28-MO (atg and spl) were injected at 4ng per blastomere either alone or in combination with MMP28 mRNAs at 8 cell stage, in 2 animal blastomeres for *in situ* hybridization (ISH), neural crest extraction and grafting, or 4 animal blastomeres for PCR and qPCR. Nuclear mCherry[24] was injected at 10 pg per blastomere. Twist and Cadherin-11 mRNA were injected at 125 pg per blastomere.

In situ hybridization

Embryos were fixed overnight at 4°C in MEMFA and dehydrated by several washes in methanol. Embryos were then rehydrated by solutions of decreasing methanol concentration, washed in PBS and bleached in hydrogen peroxide (10%) to attenuate the ectoderm pigmentation. After bleaching, a short post-fixation in formaldehyde 3.7% was performed. Embryos were then processed using the InsituPro VS (Intavis AG Bioanalystical Instruments, Germany) automate. Briefly, embryos were incubated 16 hours at 65°C in formamide-based hybridization buffer containing a digoxigenin or Fluorescein-12-labelled antisense probe against the gene of interest. Probes were washed in formamide-based washing solutions, then washed in PBS plus 0.1% tween, and sequentially incubated for 1 hour in a serum-based blocking solution and then for 1 hour in blocking solution containing the anti-digoxigenin (Roche, 11093274910, 1/2000) or anti-Fluorescein (Roche 11426346910, 1/10000) antibody coupled with alkaline phosphatase. Staining was performed by incubating embryos in staining buffer (pH9.5) containing NBT (Promega, S380C) at 50µg/mL and BCIP (Promega, S381C) at 100 µg/mL or Magenta-Phos (Biosynth, B-7452). The following probes were used: XL-snai2[45], XL-twist1[46], XL-MMP28[23], XL-foxD3[47], XL-snai1[48], XL-sox8[49], XL-sox9[50], XL-sox10[51], XL-eya1[52], XL-six1[53], XL-foxi4.1[54], XL-sox2[55], XL-keratin[56], XL-pax3[57].

Ex-vivo neural crest culture

NC cultures were performed as described elsewhere[25]. Briefly, neural crest explants were isolated from stage 18 embryos using a hair knife (hair mounted on a glass pipette) and plated on fibronectin-coated Ibidi µslides dishes (Ibidi, ref 80821). Dishes were prepared by incubating fibronectin solution at 10 µg/mL for one hour at 37ºC.

Grafts of Neural Crest cells

Grafts were performed as described elsewhere[33]. Embryos at stage 18 were immobilized into a Petri dish filled with modelling clay. The pigmented ectoderm layer located above the neural crest region was carefully removed. Neural crest cells were mechanically detached from their surrounding tissues by applying gentle pressure on the side of the neural crest domain in a lateral to medial direction. To perform the graft, a given neural crest explant was first dissected out from a host embryo, then a neural crest explant was harvested from the donor embryo and grafted into the wound of the host and kept in place by a piece of glass coverslip for 15 min. The coverslip is then removed and embryos are left to heal.

Immunostaining on cell cultures

Xenopus NC cells were cultured on fibronectin-coated dishes and were allowed to migrate for a few hours, fixed in PFA 4% for 30 minutes, blocked and permeabilized (PBS1X, 2% serum and 0.1% Triton) for 30 minutes and incubated 2 hours at room temperature or overnight at 4°C with a primary antibody. After several washes in PBS, they were incubated 1 hour at room temperature or overnight at 4°C with a secondary antibody mixed with DAPI and/or Phalloidin, and analysed on a Zeiss 710 inverted confocal microscope. Primary antibodies: Rabbit anti-GFP (Torrey Pines BioLabs, TP-401; 1:200), Rabbit anti-Flag (MilliporeSigma, F1804; 1:200). Secondary antibodies: goat anti-rabbit Alexa-488 or 555 (ThermoFisher Scientific).

qPCR and PCR

Total RNAs from neural crest explants from injected embryos were extracted with RNeasy® Micro Kit (Qiagen) and used for relative quantitative PCR (QuantStudio 3 real Time PCR system; ThermoFisher scientific) using Power SYBR™ Green RNA-to-C_T 1-Step Kit according to the manufacturer instructions. The following primers set were used:
Cadherin-11_rev: 5'-CATCCTCTGGGTTGATGCTG 3',
Cadherin-11_fwd: 5'-TCGGATACTGTGGTCGGAAG-3',
N-cadherin_rev: 5'-ATTGTAACGGAGACGGTTGC-3',
N-cadherin_fwd: 5'-CAGCAACGATGGCTTAGTGA-3',
XB-cadherin_fwd: 5'-TATCCTTGCTGCTGCTCCTG-3',
XB-cadherin_rev: 5'-TCACCTCCACCTTCCTCTCC-3',
E-cadherin_rev: GCACAGAGCCTTCAAAGACC-3',
E-cadherin_fwd: 5'-CGACCTTTGGACAGAGAAGC-3',
EeF1a1_rev: 5'-CACGGGTTTGTCCATTCTTT-3',
EeF1a1_fdw: 5'-ATTGATGCTCCAGGACACAG-3',
Twist1qPCR_fdw: 5'-CGACTTTCTCTGCCAGGTCT-3',
Twist1qPCR_rev: 5'-TCCACACGGAGAAGGCATAG-3',
MMP28-E7_fdw: 5'-TGCAGTGGTATCGGGTTTAG-3',
MMP28-E8_rev: 5'-AAAGTGCAGTGTCAGGACGA-3',
Sox10_fdw: 5'-CTGTGAACACAGCATGCAAA-3'
Sox10_rev: 5'-TGGCCAACTGACCATGTAAA-3',
MMP28-E1_fdw: 5'-GGAAGCTGCTATTCCATCCCTGT-3',
MMP28-E1_rev: 5'-ACCTGTGCAGTTTGTAGGGTCT-3',
Six1_fdw: 5'-CTGGAGAGCCACCAGTTCTC-3',
Six1_rev: 5'-AGTGGTCTCCCCCTCAGTTT-3'.
All pair of primers were validated using the standard curve method, and the data were normalized to EEF1α.

For Morpholino validation by RT-PCR, total RNAs from injected embryos were extracted with RNeasy® Micro Kit (Qiagen) and reverse-transcribed using SuperScript™ IV VILO™ Master Mix (ThermoFisher Scientific, #11756050) according to the manufacturer instructions, and used for PCR with Illustra™ PuReTaq Ready-To-Go™ PCR beads. The following primer sets were used:
ODC_fdw: 5'-ACATGGCATTCTCCCTGAAG-3',
ODC_rev: 5'-TGGTCCCAAGGCTAAAGTTG-3',

MMP28-E1b_fdw: 5'-GAAGAGACCCTACAAACTGC-3',
MMP28-E8_rev: 5'-AAAGTGCAGTGTCAGGACGA-3',
MMP28-I1-rev: 5'-GACAACGCATTTCCCAAACT-3',

Statistics

Comparison of percentages was performed using contingency tables[58]. Two data sets were considered significantly different (null hypothesis rejected) if $T > 3.841$ ($\alpha = 0.05$, *), $T > 6.635$ ($\alpha = 0.01$, **) or $T > 10.83$ ($\alpha = 0.001$, ***). Normality of data sets was tested using Kolmogorov-Smirnov's test, d'Agostino and Pearson's test and Shapiro-Wilk's test using Prism6 (GraphPad). A data set was considered normal if found as normal by all three tests. Datasets following a normal distribution were compared with Student T-test (two-tailed, unequal variances) or a one-way ANOVA with multiple comparisons post-test in Prism6 (GraphPad). Datasets that did not follow a normal distribution were compared using Mann Whitney's test or a non-parametric ANOVA using Prism6 (GraphPad). Cross-comparisons were performed only if overall P value of the ANOVA was < 0.05. Strategy for sample size determination does not apply here since all embryos or cells available were analysed. Statistics were performed on the whole population. Variances were not assumed to be equal. Box and whiskers plot: the box extends from the 25th to the 75th percentile; the whiskers show the extent of the whole dataset. The median is plotted as a line inside the box. Statistics are provided in figure legends or added directly onto the graphs. All error bars on graphs and curves that are not box and whiskers plots correspond to the standard deviation (s.d) or standard error of the mean (s.e.m) as indicated in the figure legends.

Image analysis

The net distance of *in vivo* NC cells migration was measured using FIJI/Image J by drawing a straight line between the dorsal midline and the ventral-most NC cells of each stream. The mean length of dorsoventral extension is calculated per embryo and each side (experimental vs control/non-injected). The ratio of the mean dorsoventral extension is plotted after normalization to the control condition of reference.

Neural crest areas at pre-migratory stages were measured as follows: ISH images were converted to 32-bit black and white (NBT/BCIP magenta staining being white on a black background), thresholded with background converted to NaN, automatic measurements of area were made with batch processing in FIJI/imageJ. If an embryo had too much background after ISH, the size of the NC area was retrieved by hand in FIJI/ImageJ using the polygon tool.

Analysis of nuclear localization of the various MMP28-GFP constructs was performed from 3D confocal stacks with optimal pinhole settings acquired after immunostaining against GFP and counterstaining with DAPI. In Imaris (Bitplane), the DAPI channel was used as a mask to sample the GFP channel. Then, surface analysis was performed to calculate the volume of the nuclei and the volume of the GFP within the nuclei. Nuclear localization is expressed as a ratio between the volume of nuclear GFP immunostaining and the nuclear volume.

Bioinformatics analysis of Xenopus MMP28 protein sequence

Xenopus laevis MMP28 amino acid sequence was searched for putative importin α-dependent nuclear localization signals and nuclear export signals using cNLS mapper[59] (http://nls-mapper.iab.keio.ac.jp/cgi-bin/NLS_Mapper_form.cgi) and ValidNESs[60] (http://validness.ym.edu.tw/).

Western Blots

Cell fractions of fifty (100 mg) stage 17 wild-type or injected embryos were obtained using the Subcellular Protein Fractionation Kit for Tissues (ThermoFisher Scientific # 87790). Protein quantification was performed using Bradford technique (Pierce). Around 40 µg of proteins were loaded per lane of a 4-12% precast gel (Bio-Rad Mini-PROTEAN®). Proteins were transferred on PVDF-membrane and blocked for 1h with 5% skimmed milk. Anti-GFP 1:1000 (Torrey Pines BioLabs; TP-401), anti-Tubulin 1:1000 (Sigma, T9026), anti-rabbit-HRP or anti-mouse-HRP 1:10000 (Millipore; catalog #).

Methods references

24 Mayor, R., Morgan, R. & Sargent, M. G. Induction of the prospective neural crest of *Xenopus*.*Development* **121**, 767-777 (1995).

25 Hopwood, N. D., Pluck, A. & Gurdon, J. B. A *Xenopus* mRNA related to Drosophila twist is expressed in response to induction in the mesoderm and the neural crest. *Cell* **59**, 893-903 (1989).

26 Monsoro-Burq, A. H., Fletcher, R. B. & Harland, R. M. Neural crest induction by paraxial mesoderm in *Xenopus* embryos requires FGF signals. *Development* **130**, 3111-3124, doi:10.1242/dev.00531 (2003).

27 Essex, L. J., Mayor, R. & Sargent, M. G. Expression of *Xenopus* snail in mesoderm and prospective neural fold ectoderm. *Developmental dynamics : an official publication of the American Association of Anatomists* **198**, 108-122, doi:10.1002/aja.1001980205 (1993).

28 O'Donnell, M., Hong, C. S., Huang, X., Delnicki, R. J. & Saint-Jeannet, J. P. Functional analysis of Sox8 during neural crest development in *Xenopus*. *Development* **133**, 3817-3826, doi:10.1242/dev.02558 (2006).

29 Spokony, R. F., Aoki, Y., Saint-Germain, N., Magner-Fink, E. & Saint-Jeannet, J. P. The transcription factor Sox9 is required for cranial neural crest development in *Xenopus*. *Development* **129**, 421-432 (2002).

30 Aoki, Y. *et al.* Sox10 regulates the development of neural crest-derived melanocytes in *Xenopus*. *Developmental biology* **259**, 19-33, doi:10.1016/S0012-1606(03)00161-1 (2003).

31 David, R., Ahrens, K., Wedlich, D. & Schlosser, G. *Xenopus* Eya1 demarcates all neurogenic placodes as well as migrating hypaxial muscle precursors. *Mechanisms of development* **103**, 189-192, doi:10.1016/s0925-4773(01)00355-0 (2001).

32 Ghanbari, H., Seo, H. C., Fjose, A. & Brandli, A. W. Molecular cloning and embryonic expression of *Xenopus* Six homeobox genes. *Mechanisms of development* **101**, 271-277, doi:10.1016/s0925-4773(00)00572-4 (2001).

33 Schlosser, G. & Ahrens, K. Molecular anatomy of placode development in *Xenopus* laevis. *Developmental biology* **271**, 439-466, doi:10.1016/j.ydbio.2004.04.013 (2004).

34 Mizuseki, K., Kishi, M., Matsui, M., Nakanishi, S. & Sasai, Y. *Xenopus* Zic-related-1 and Sox-2, two factors induced by chordin, have distinct activities in the initiation of neural induction. *Development* **125**, 579-587 (1998).

35 Jonas, E., Sargent, T. D. & Dawid, I. B. Epidermal keratin gene expressed in embryos of *Xenopus* laevis. *Proceedings of the National Academy of Sciences of the United States of America* **82**, 5413-5417, doi:10.1073/pnas.82.16.5413 (1985).

36 Bang, A. G., Papalopulu, N., Kintner, C. & Goulding, M. D. Expression of Pax-3 is initiated in the early neural plate by posteriorizing signals produced by the organizer and by posterior non-axial mesoderm. *Development* **124**, 2075-2085 (1997).

37 Gouignard, N., Rouviere, C. & Theveneau, E. in *Epithelial-Mesenchymal Transition Methods in Molecular Biology* (eds K. Campbell & E. Theveneau) (Springer, 2020, IN PRESS).

38 Bajanca, F. *et al. In vivo* topology converts competition for cell-matrix adhesion into directional migration. *Nature communications* **10**, 1518, doi:10.1038/s41467-019-09548-5 (2019).

39 Taillard, E. D., Waelti, P. & Zuber, J. Few statistical tests for proportions comparison. *Eur J Oper Res* **185**, 1336-1350, doi:10.1016/j.ejor.2006.03.070 (2008).

Acknowledgements
The authors are grateful to Profs. Marianne Bronner (CalTech) and A-H Monsoro-Burq (Institut Curie, College de France) as well as Drs Bertrand Benazeraf (CNRS, University of Toulouse), Kyra Campbell (Sheffield University), Guojun Sheng (Kumamoto University), Sei Kuriyama (Akita University), Ben Steventon (Cambridge University) for critical reading of the manuscript and friendly advice. E.T. acknowledges support from the French National Center for Scientific Research (CNRS), the Fondation pour le Recherche Medicale (FRM AJE201224), the Midi-Pyrenees Regional Council (13053025), Toulouse Cancer Sante (DynaMeca) and Universite Paul Sabatier. N.G was supported by grants from the Fondation pour le Recherche Medicale (ARF20150934153), the European Marie Curie Prestiges Program (PRESTIGES 2015–4–007), a grant from the National Institutes of Health (R21 DE029333) and a pilot grant from the NYU Center for Skeletal and Craniofacial Biology which was established by NIH (1P30DE020754). J-P. S-J. acknowledges support from a grant from the National Institutes of Health (R01DE25806).

Author contributions
E.T. supervised the project. N.G., J-P. S-J., A.B. and E.T. designed and performed the experiments in *Xenopus* laevis. N.G., J-P. S-J. and E.T. analysed the data. N.G. and E.T. organized the figures and supplementary materials. E.T. wrote the article with the participation of N.G. and J-P. S-J.

Competing interest declaration
The authors declare no competing interests.

Correspondence and requests for materials should be addressed to E.T.
eric.theveneau@univ-tlse3.fr